# The first 8-13 $\mu$m spectra of AGB stars in the Magellanic Clouds


M. A. T. Groenewegen

*Institut d'Astrophysique de Paris, CNRS, 98bis Boulevard Arago, F-75014 Paris, France*

C. H. Smith

*Dept. of Physics, University College, ADFA, Canberra ACT 2600, Australia*

P. R. Wood

*Mount Stromlo and Siding Springs Observatories, Private Bag, Weston Creek P.O., Canberra ACT 2611, Australia*

A. Omont

*Institut d'Astrophysique de Paris, CNRS, 98bis Boulevard Arago, F-75014 Paris, France*

T. Fujiyoshi

*Dept. of Physics, University College, ADFA, Canberra ACT 2600, Australia*



## ABSTRACT

We have obtained 8-13 $\mu$m spectra of two AGB stars in the Magellanic Clouds (MCs), and report the first detection of dust features in AGB stars in the MCs. The long period variable (LPV) TRM60 (P = 1260 days) in the LMC displays silicate absorption, and the LPV GM103 (P = 1070 days) in the SMC shows silicate emission. The presence of silicates confirms previous observations using different techniques that these stars are oxygen-rich. By modeling the spectral energy distributions and 8-13 $\mu$m spectra with a dust radiative transfer model we find that although the two stars have similar high luminosities their dust optical depths differ by a factor of 10.

A similar analysis was carried out for a Galactic OH/IR star of comparable period. The results for these three stars suggest that the mass loss rate increases with metallicity in AGB stars.



*Subject headings:* circumstellar matter – stars: mass loss – stars: AGB and post-AGB – Infrared: stars

## 1. Introduction

Searches for Asymptotic Giant Branch (AGB) stars in the Magellanic Clouds (MCs) have been made using optical spectroscopic surveys (e.g. Blanco et al. 1980, Blanco & McCarthy 1991, Rebeirot et al. 1991), photometric surveys using V and I Schmidt plates (e.g. Reid et al. 1987) and optical surveys for LPVs (e.g. Payne-Gaposhkin 1971; Hughes 1989). However, these surveys failed to identify the red dust-enshrouded OH/IR stars and infrared carbon stars in the MCs, very luminous examples of which did turn up in the IRAS point source catalog. Recently, near-infrared studies have been initiated to study IRAS sources in the MCs (Reid et al. 1990, Reid 1991, Wood et al. 1992 (W92), Zijlstra et al. 1995). From NIR data alone it is almost impossible to distinguish between an oxygen- and a carbon-rich dust enshrouded object. To determine the chemical type of obscured stars one can use narrow-band 10 $\mu$m photometry (Zijlstra et al. 1995) or look for OH emission (e.g. W92). A direct way is to observe the 8-13 $\mu$m region and look for the 9.8 $\mu$m silicate or 11.3 $\mu$m silicon carbide dust feature.

Here we report on the detection of the silicate dust feature in one LMC and in one SMC AGB star. We model the spectral energy distributions (SEDs) and 8-13 $\mu$m spectra and determine the luminosity and (dust) mass loss rate.

## 2. Observations

The data were taken on November 25-27, 1994 with the UCL IR cooled grating array spectrometer (for details see Aitken & Roche 1982) mounted at the f/36 Cassegrain focus of the 3.9m Anglo-Australian Telescope. We used a circular aperture of 4.2$''$ diameter, while the (optical) seeing was in the range 1.0-1.5$''$ for most of the time. The 8.0 to 13.0 $\mu$m window was covered with 25 detectors, resulting in an effective resolution of $\lambda/\Delta\lambda \approx 50$. The grating was stepped once, offset by one and a half detector widths, providing an oversampled (50 data point) spectrum, which was subsequently smoothed. Chopping, with a frequency of 12.5 Hz, and beam-switching were employed, each using a throw of 15$''$ in declination. The pointing of the telescope was regularly verified on a bright nearby star. The observations were obtained through cirrus clouds which is reflected by the large error bars. Flux calibration and correction for telluric absorption were made by reference to the F0II star $\alpha$ Car.

We observed 9 objects but only detected TRM60 (IRAS 05529-6708) and GM103 (see Table 1). The non-detection of the the others is most likely due to variability since it turns out that the two stars detected were observed near maximum light.

The spectra of TRM60 and GM103 are shown in Figs. 1 and 2. The on-source integration times are 21.3 and 32 minutes, respectively. The spectrum of GM103 clearly indicates silicate emission, while that of TRM60 possibly suggests silicate absorption, although the S/N is poor.

## 3. Modelling

Since both stars are long period variables (LPVs) it is important to use photometry taken as close as possible in phase to the AAT observations. Based on the periods and the time of maximum light (W92, Wood et al. 1995 (W95)) the AAT observations of TRM60 are obtained at phase 0.13 and those of GM103 at phase 0.95. From W92 for TRM60 and W95 for GM103 we took JHK(L$'$) photometry closest in phase to the AAT observations. The magnitudes are listed in Table 1 which include 'error bars' indicating the change in magnitudes over roughly 0.05 in phase from the adopted photometry. In addition we list the IRAS 12 and 25 $\mu$m flux-densities from the IRAS Faint Source Catalog (FSC; TRM60) and Schwering & Israel (1989; GM103). The SEDs and 8-13 $\mu$m spectra were modeled using the model of Groenewegen (1993) assuming a r$^{-2}$ density distribution. For the central star the theoretical model flux of a M4 star is used (Fluks et al. 1994; $T_{\rm eff}$ = 3490 K). Changing the flux from an M4 star to that of a 2500 K blackbody does not change the results significantly; the effects are largest for GM103 which has a lower mass loss rate (see Table 2). The silicate dust opacity of Volk & Kwok (1988; VK) and a combination of dirty silicate (Jones & Merrill 1976) and the silicate feature of David & Papoular (1990) (JMDP) are used. The inner dust radius is determined by imposing a condensation temperature of the dust of $T_{\rm c}$ = 1000 K. Luminosities are determined by adopting a distance to the LMC of 50 kpc, and to the SMC of 60 kpc. A foreground extinction of $A_{\rm V}$ = 0.1 is assumed.

The best fits are shown in Figs. 1 and 2 with model parameters listed in Table 2. We recall that the fitting process only fixes the dust optical depth, which is related to physical parameters in the present model by $\tau_\lambda \sim (\dot{\rm M}\, \Psi\, \kappa_\lambda)/(R_\star\, r_{\rm inner}\, v)$ where $\dot{\rm M}$ is the total

| Name | Period (days) | Position (1950) | J | H | K | $L'$ | $S_{12}$ (Jy) | $S_{25}$ (Jy) |
|---|---|---|---|---|---|---|---|---|
| TRM 60 | 1260 | 5h32m55.2s $-67$d08′49″ | 14.90 ± 0.30 | 11.66 ± 0.17 | 9.48 ± 0.20 | 7.18 ± 0.26 | 1.09 | 1.59 |
| GM 103 | 1070 | 0h48m44.1s $-73$d07′50″ | 10.11 ± 0.10 | 9.10 ± 0.15 | 8.57 ± 0.20 | – | 0.44 | 0.89 |

Table 1: Observed parameters

| Name | Dust[a] | Star[b] | Lum. ($L_\odot$) | $\tau_{9.X}$[c] | $\tau_{0.5}$[d] | $\dot{M}$[e] ($M_\odot$/yr) |
|---|---|---|---|---|---|---|
| TRM60 | VK | M4 | 58000 | 4.1 | 18.2 | 1.1 $10^{-5}$ |
| TRM60 | JMDP | M4 | 54000 | 7.6 | 11.9 | 6.0 $10^{-5}$ |
| TRM60 | VK | BB | 55000 | 4.2 | 18.7 | 1.0 $10^{-5}$ |
| TRM60 | JMDP | BB | 55000 | 7.8 | 12.2 | 5.8 $10^{-5}$ |
| | | | | | | |
| GM103 | VK | M4 | 81000 | 0.44 | 1.93 | 3.3 $10^{-6}$ |
| GM103 | JMDP | M4 | 84000 | 0.74 | 1.16 | 1.8 $10^{-5}$ |
| GM103 | VK | BB | 81000 | 0.20 | 0.87 | 1.3 $10^{-6}$ |
| GM103 | JMDP | BB | 76000 | 0.36 | 0.56 | 7.0 $10^{-6}$ |
| | | | | | | |
| OH138 | VK | M4 | 2160[f] | 6.4 | 28.3 | 2.0 $10^{-6}$[g] |
| OH138 | JMDP | M4 | 2040[f] | 7.9 | 12.4 | 7.3 $10^{-6}$[g] |
| OH138 | JMDP | M4 | 870[f] | 12.2 | 19.1 | 8.0 $10^{-6}$[g] |

Table 2: Model results

[a] VK = Volk & Kwok (1988); JMDP is a combination of dirty silicate (Jones & Merrill 1976) and the silicate feature of David & Papoular (1990).

[b] The flux of the central star is either the flux of a M4 star with an effective temperature of 3490 K or a 2500 K blackbody.

[c] Optical depth at the peak of the silicate feature which occurs at 9.7 $\mu$m for VK dust and at 9.9 $\mu$m for JMDP dust.

[d] Dust optical depth at 0.5 $\mu$m.

[e] Total mass loss rate, calculated from the optical depth, assuming a dust-to-gas ratio of $\Psi = 0.003$ (TRM60), 0.001 (GM103), 0.004 (OH138) and $v$ = 12 km s$^{-1}$ (TRM60, GM103) or 9.4 km s$^{-1}$ (OH138; see Herman & Habing 1985).

[f] Luminosity ($L_\odot$)/(distance (kpc))$^2$

[g] mass loss rate /distance ($M_\odot$/yr/kpc)

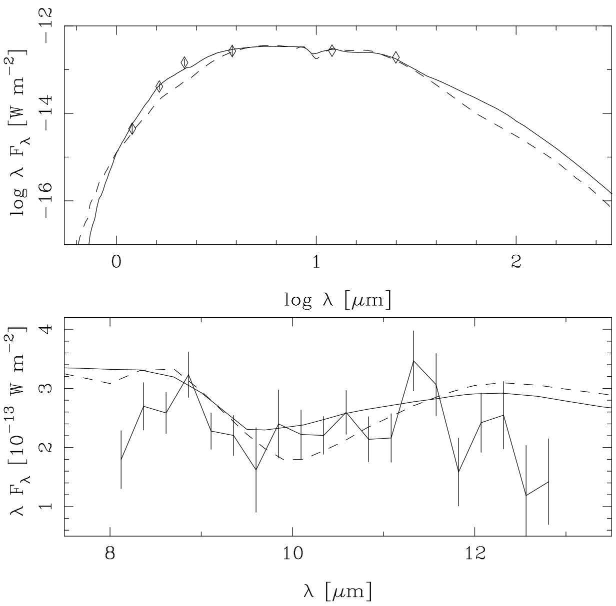


Fig. 1.— TRM60. The solid line represents the best fitting model with VK-dust, the dashed line that with JMDP-dust. The observed broadband photometry and IRAS fluxes are indicated by the diamonds.

mass loss rate, $\Psi$ the dust-to-gas ratio, $\kappa_\lambda$ the dust opacity, $R_\star$ the stellar radius in solar radii, $r_{\rm inner}$ the inner dust radius in stellar radii and $v$ the expansion velocity of the envelope.

The SEDs and mid-ir spectra are fitted well in general. For TRM60 the VK dust gives an overall better fit to the SED. For GM103, the VK dust gives a better fit to the 8-13 $\mu$m spectra if the models are scaled to the continuum. From the fit to GM103 is is obvious that the IRAS 25 $\mu$m point (0.89 Jy) lies well above the predicted model flux-density (0.31-0.38 Jy). We inspected two-dimensional images and one-dimensional co-adds of IRAS scans using the GIPSY software package (Wesselius et al. 1992). At 25 $\mu$m, the one-dimensional co-add clearly indicates the source is not a point source. It is not clear however whether the source is physically extended. The IRAS image shows that there are two very red, strong 25 $\mu$m emitters (00489$-$7305 and 00478$-$7305) at less than $5.2'$ from GM103. Since the size of the 25 $\mu$m detector on the sky is $0.75' \times 4.7'$ it is likely that emission from one or both of these nearby sources contaminates the published 25 $\mu$m flux of GM103. We also find that GM103 is a point source at 12 $\mu$m, as is TRM60 at 12 and 25 $\mu$m.

We derive luminosities at the time of observation of about 55000 and 80000 $L_\odot$ for TRM60 and GM103 respectively, above the classical upper limit of about 54000 $L_\odot$ ($M_{\rm bol} = -7.1$), raising the question on the AGB character of the two stars. However, both stars are observed close to maximum light and based on published photometry (W92, W95) and model fitting we estimate mean luminosities of 46500 and 51000 $L_\odot$ for TRM60 and GM103, respectively, within the range expected for massive AGB stars. In addition, TRM60 and GM103 are large-amplitude variables ($\Delta K$ = 1.9 and 1.5 magnitudes, respectively) which are not observed among supergiants (Wood et al. 1983).

In the last column of Table 2 we list the mass loss rate, assuming $v$ = 12 km s$^{-1}$ and a dust-to-gas ratio of $\Psi = 0.003$ (TRM60) and 0.001 (GM103). The expansion velocity of 12 km s$^{-1}$ for TRM60 is determined from the OH line profile (W92); for GM103 we simply assume the same value, although one may expect a lower value. That the two types of silicates give so different mass loss rates (for fixed $v$ and $\Psi$) is due to the difference in dust opacity: $\kappa_{60}$ = 1910 cm$^2$g$^{-1}$ for VK dust and 134 cm$^2$g$^{-1}$ for JMDP dust. The value for VK dust is significantly larger than usually quoted for silicate dust (150 cm$^2$g$^{-1}$, Jura 1986, or 108 cm$^2$g$^{-1}$, Schutte & Tielens 1989).

Independent of the uncertainty in $v$, $\Psi$ or $\kappa_\lambda$ the major conclusion of the model fitting is that a LMC and a SMC AGB star of comparable luminosity and pulsation period differ in dust optical depth by a factor of 10. This result is consistent with the observation of Wood et al. (1992) that the SMC contains two known luminous AGB stars with P > 1000 days and both are optically visible, while all known stars of this type in the LMC are deeply dust enshrouded and optically invisible.

## 4. Discussion and conclusions

The detection of the silicate feature classifies TRM60 and GM103 as being oxygen-rich, and it demonstrates the usefulness of 8-13 $\mu$m spectroscopy as a tool to classify AGB stars. For both stars the oxygen-rich character was determined previously by other means. W95 detected TiO bands in an optical spectrum of GM103, while W92 detected OH mase emission in TRM60.

As TRM60 and GM103 with roughly the same period and luminosity have very different dust optical depths, the question arises if this is due to a difference in metallicity. In order to make the comparison we selected an oxygen-rich Mira in the Galaxy, the OH/IR star 138.0+7.3 (= IRAS 03206+6521; short OH138) with a period of 1276 days (van Langevelde et al. 1990) comparable to those of TRM60 and GM103. Broad-band photometry was taken from Noguchi et al. (1993) and Jiang & Hu (1992). In addition, Smith & Herman (1990) presented near-simultaneous 8 - 13 and 2.8 - 3.6 $\mu$m spectra. The SED and LRS spectrum of this star are fitted in the same way as the MC stars. Interstellar extinction of $A_{\rm V}$ = 3.0 is adopted, based on Neckel & Klare (1980) and Burstein & Heiles (1982). The best fitting models are presented in Fig. 3 with parameters listed in Table 2.

Contrary to the two MC stars the best fit to both the SED and the LRS spectrum (in particular the location of the minimum at 10 $\mu$m) is obtained with JMPD dust. This may hint to a different type of silicate dust in the MCs possibly related to a different chemical composition.

From a comparison of three stars of comparable pulsation period in the (outer) Galaxy, the LMC and the SMC we derive that the dust optical depths have ratios of Galaxy : LMC : SMC $\approx$ 15 : 10 : 1. This is in all likelihood due to a difference in metallicity. If we assume that $\Psi \sim Z$ (the dust-to-gas ratio proportional to the material that can condense into grains) and that the luminosity of OH138 near maximum light is also in the range 55000 - 80000 $L_{\odot}$ then we find a ratio of the mass loss rates of 4 : 3 : 1. This suggests that the mass loss rate in AGB stars increases with metallicity. This is the first time that the relation between mass loss and metallicity is quantified for AGB stars.

Although we present the first detections of silicate dust features in AGB stars outside of our Galaxy, these observations also reveal the limitations of present-day ground-based observations. Even on a 4m class telescope the limiting flux-density for which useful spectra can be obtained during summer on the southern hemisphere limits the usefulness to only the very brightest AGB stars in the MCs. In the near future the ISO mission will provide useful spectra for selected AGB stars in the MCs. For an order of magnitude improvement in ground-based observations from the southern hemisphere one likely has to wait for MIIS (Mid-Infrared Imager/Spectrometer) on the VLT (Moorwood 1994) to be commissioned.

The observing trip of M.G. to the Anglo-Australian Telescope and his subsequent stay at ADFA were made possible by financial support from the Franco-Australian fund for scientific collaboration.

## REFERENCES

Aitken D.A., Roche P.F., 1982, MNRAS 200, 217

Blanco V.M., McCarthy M.F., Blanco B.M., 1980, ApJ 242, 938

Blanco V.M., McCarthy M.F., 1991, AJ 100, 674

Burstein D., Heiless C., 1982, AJ 87, 1165

David P., Papoular R., 1990, A&A 237, 425

Fluks M.A., Plez B., Thé P.S., de Winter D., Steenman H.C., Westerlund B.E., 1994, A&AS 105, 311

Groenewegen, M.A.T., 1993, Ph.D. Thesis, Chapter 5, University of Amsterdam

Herman J., Habing H.J., 1985, A&AS 59, 523

Hughes S.M.G., 1989, AJ 97, 1634

Jiang B.-W., Hu J.-Y., 1992, Chin. Astron. Astrophys. 16, 416

Jones T.W., Merrill K.M., 1976, ApJ 209, 509

Jura M., 1986, ApJ 303, 327

Moorwood A.F.M., 1994, in: Infrared astronomy with arrays: the next generation, Ed. I.S. McLean, Kluwer academic publishers, p. 465

Neckel Th., Klare G., 1980, A&AS 42, 251

Noguchi K., Qian Z., Wang G., Wang J., 1993, PASJ 45, 65

Payne-Gaposhkin C.H., 1971, Smithsonian Contr. Ap. 13, 1

Rebeirot E., Azzopardi M., Westerlund B.E., 1991, A&AS 97, 603

Reid N., 1991, ApJ 382, 143

Reid N., Mould J., Thompson I., 1987, ApJ 323, 433

Reid N. Tinney C., Mould J., 1990, ApJ 348, 98

Schutte W.A., Tielens A.G.G.M., 1989, ApJ 343, 369

Schwering P.B.W., Israel F.P., 1989, A&AS 79, 79

Smith R.G., Herman J., 1990, A&A 227, 147

van Langevelde H.J., van der Heiden R., Schooneveld C., 1990, A&A 239, 193

Volk K., Kwok S., 1988, ApJ 331, 435

Wesselius P.R., de Jonge A.R.W., Kester D.J.M. and Roelfsema P.R., 1992, in "Infrared Astronomy with ISO", eds. T. Encrenaz and M.F. Kessler, Nova Science Publishers Inc. NY., p. 509

Wood P.R., Bessell M.S., Fox M.W., 1983, ApJ 272, 99

Wood P.R., Whiteoak J.B., Hughes S.M.G., Bessell M.S., Gardener F.F., Hyland A.R., 1992, ApJ 397, 552 (W92)

Wood P.R., Moore G.M., Bessell M.S., 1995, in preparation (W95)

Zijlstra A.A., Loup C., Waters L.B.F.M., Whitelock P.A., Guglielmo F., 1995, A&A, submitted/preprint

This 2-column preprint was prepared with the AAS LaTeX macros v3.0.

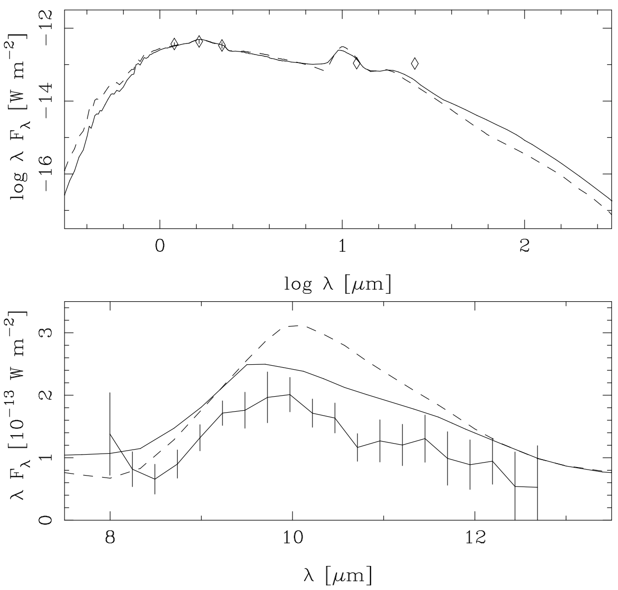


Fig. 2.— As Fig. 1 for GM103.

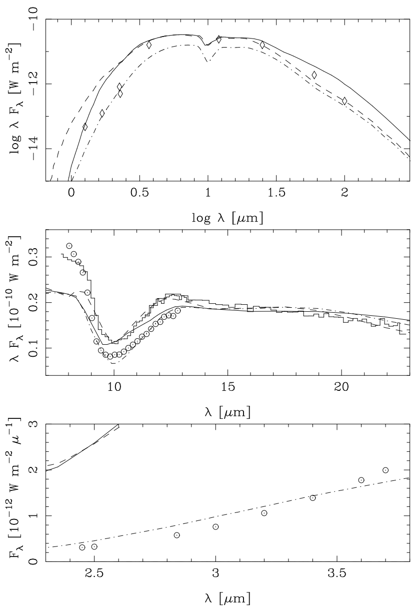


Fig. 3.— OH138+7.3. The solid line represents the best model with VK-dust, the dashed line that with JMDP-dust, fitted to the IRAS data. The observed broadband photometry and IRAS fluxes are indicated by diamonds. The 2 - 4 and 8 - 13 $\mu$m spectra (circles) are from Smith & Herman (1990). The plotted 8-13 $\mu$m spectrum is the observed one multiplied by 4.5. Since the 2.4 - 2.5 and 2.8 - 3.7 $\mu$m spectra are featureless only the start and end, and some intermediate points are plotted. The dot-dashed line is the best model fitted to the 2-4 $\mu$m spectrum with JMDP dust. In the middle panel all models are scaled to the observed LRS spectrum near 15 $\mu$m.